ACES Asian Chemical Editorial Society

doi.org/10.1002/asia.202300290

CHEMISTRY AN ASIAN JOURNAL Review

www.chemasianj.org

Catenane and Rotaxane Synthesis from Cucurbit[6]uril-Mediated Azide-Alkyne Cycloaddition

Yuen Cheong Tse[a] and Ho Yu Au-Yeung*[a, b]

The chemistry of mechanically interlocked molecules (MIMs) such as catenane and rotaxane is full of new opportunities for the presence of a mechanical bond, and the efficient synthesis of these molecules is therefore of fundamental importance in realizing their unique properties and functions. While many different types of preorganizing interactions and covalent bond formation strategies have been exploited in MIMs synthesis, the use of cucurbit[6]uril (CB[6]) in simultaneously templating macrocycle interlocking and catalyzing the covalent formation of the interlocked components is particularly advantageous in accessing high-order catenanes and rotaxanes. In this review, catenane and rotaxane obtained from CB[6]-catalyzed azide-alkyne cycloaddition will be discussed, with special emphasis on the synthetic strategies employed for obtaining complex [n]rotaxanes and [n]catenanes, as well as their properties and functions.

1. Introduction

Catenane and rotaxane are two archetypical classes of mechanically interlocked molecules (MIMs) characterized by the presence of physically entangled, or mechanically bonded, molecular components (Figure 1).[1] While being interlocked in the same molecular framework, the constituting macrocycles and dumbbells are not covalently restricted and hence could undergo large-amplitude motions, and catenane- and rotaxane-based molecular switches and machines can therefore be constructed when these motions are designed to be triggered by external stimuli. In addition, the unique properties associated to the dynamics, structures, topology and stereochemistry as a result of the mechanical interlocking also render these MIMs highly promising in many other areas such as host-guest chemistry,[2] sensing,[3] controlled-delivery,[4] catalysis,[5] smart material[6] and etc. Synthetic methods for obtaining catenane and rotaxane in high yields and diverse structures are therefore essential for fully exploiting the unique potential of MIMs.

Template-directed synthesis is one of the most widely used strategies in the preparation of MIMs, in which precursor molecules are first preorganized by reversible non-covalent interactions and subsequently the entanglement is locked in space by covalent bond formation. Therefore, both the templating efficiency and choice of the covalent bond forming processes are critical to an efficient MIM synthesis. Among the various chemical reactions, click reaction, and in particular, copper(I)-catalyzed 1,3-dipolar [3+2]cycloaddition between azide and alkyne (CuAAC)[7] has been extensively applied in the preparation of MIMs by virtue of its high yielding nature, mild reaction conditions, high reaction rate and good compatibility with different functional groups. Indeed, since the discovery of CuAAC in 2002, it has become one of the most powerful tools in assisting chemists to construct a plethora of interlocked architectures with diverse functionalities.[8]

To create mechanical interlocking, macrocyclic building blocks are usually required in the preparation of MIMs. Cucurbiturils (CB), composed of glycouril units linked by methylene bridges, are a representative family of macrocycle in host-guest chemistry, in which cucurbit[6]uril (CB[6]) that contains six glycourils is perhaps the most commonly used member for guest binding and supramolecular self-assembly (Figure 2a).[9] CB[6] is structurally rigid, featuring a hydrophobic cavity and two polar portals that are each composed of six carbonyl oxygens. In addition to metal cation chelation (e.g. Na^+), the macrocycle is also a favorable host for binding organic cations (e.g. alkylammoniums), in which their hydrophobic portion and cationic charge can respectively be encapsulated in the hydrophobic cavity and bind to the preorganized carbonyl oxygens via ion-dipole interactions to result in a strong association (Figure 2b). For these favorable binding features, CB[6] is also one widely employed macrocyclic component in the construction of catenane and rotaxane,[10] in which the strong binding of CB[6] to organic ammonium building blocks has been utilized as an efficient template for creating a well-defined molecular entanglement.

In addition to simple binding, CB[6] has also been frequently exploited as supramolecular catalysts.[11] The origin of the catalytic behaviours of CB[6] has been attributed to (1) the simultaneous binding of substrates within the confined, hydrophobic cavity, leading to substantial increase in effective local concentration, and/or (2) the stabilization of the transition states.[12] The very first reaction to be catalyzed by CB[6] was discovered by Mock and co-workers in 1983, in which the macrocycle was reported to accelerate the 1,3-dipolar [3+2] cycloaddition between azidoethylammonium and propagylammonium, with an observed rate enhancement of *ca.* 10^5-fold in water.[13] Formation of the resulting triazole is highly regioselective and the 1,4-regioisomer is afforded as the sole product. Mechanistic studies revealed that the catalytic behavior is

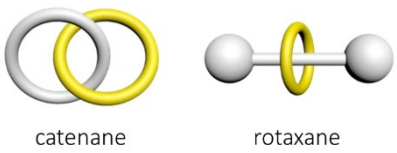

Figure 1. Schematic representation of a catenane and a rotaxane showing the interlocked components in different colours.

[a] *Dr. Y. C. Tse, Dr. H. Y. Au-Yeung*
Department of Chemistry
The University of Hong Kong
Pokfulam Road, Hong Kong (P. R. China)
E-mail: hoyuay@hku.hk

[b] *Dr. H. Y. Au-Yeung*
State Key Laboratory of Synthetic Chemistry
The University of Hong Kong
Pokfulam Road, Hong Kong (P. R. China)

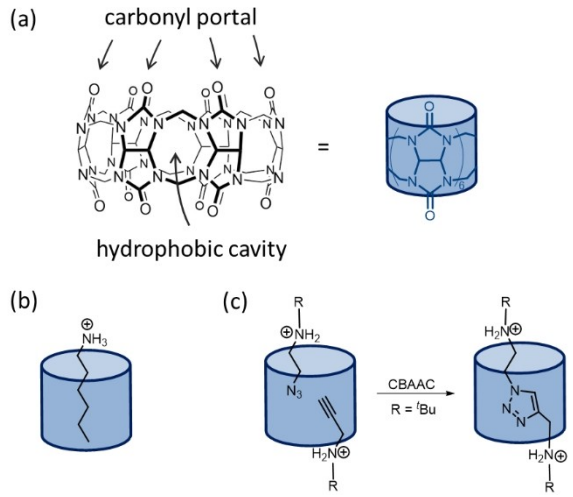

Figure 2. a) Chemical structure of CB[6], b) binding of an alkyl ammonium guest to CB[6], and c) Mock's [2]rotaxane synthesis using a CB[6]-catalyzed azide-alkyne cycloaddition (CBAAC).

related to the formation of a transient ternary complex between CB[6], azidoethylammonium and propagylammonium, in which binding of the cationic ammoniums at the carbonyl portal of CB[6] via ion-dipole interactions and hydrogen bonds extends the azide and alkyne fragments into the hydrophobic cavity of the macrocycle, releases the high-energy water molecules trapped inside the CB[6] cavity, and further stabilizes the supramolecular complex.[14] As proposed by Mock, formation of the ternary complex has two positive implications on the rate of the cycloaddition. First, this overcomes the entropic cost of bringing together the two reactants and leads to a substantial increase of the effective molarity and reaction rate. The simultaneous encapsulation of both azide and alkyne groups inside the CB[6] cavity also properly aligns the two functional motifs and leads to the regioselective formation of the 1,4-isomer. Second, strain is imposed onto both the bound azide and alkyne motifs because the CB[6] cavity is slightly undersized for perfectly accommodating the two guests, and this strain energy is relieved upon the formation of the transition state species. A computational study conducted by Maseras suggests that the effect of eliminating the entropic cost plays a more significant role than the strain relief.[15]

Based on this discovery, Mock and co-workers have also demonstrated the first example of using CB[6] to simultaneously catalyze the formation of a linear dumbbell and interlock the CB[6] to form a [2]rotaxane (Figure 2c).[14] The dual role of being a macrocyclic component and a catalyst that mediates the formation of the covalent framework of a MIM hence sets CB[6] apart from other commonly used macrocyclic hosts (e.g. cyclodextrin (CD), pillararene (PA)) in the synthesis of MIMs, demonstrating the potential of CB[6] in the efficient construction of high-order catenane and rotaxane of complex molecular architectures. In this review, the use of CB[6]-mediated azide-alkyne cycloaddition (CBAAC) in catenane and rotaxane synthesis will be discussed, and focuses will be placed on the synthesis strategies to access high-order [n]rotaxanes and [n]catenanes from CBAAC, and also their properties and functions.

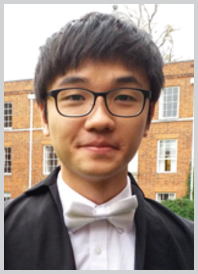

Yuen Cheong (Richard) Tse received his DPhil from University of Oxford under the supervision of Prof. Paul D. Beer, working on anion and ion-pair recognition with mechanically interlocked molecules. He was awarded a University of Oxford Croucher Scholarship for his DPhil study. Prior to this, he obtained his BSc (First Class) from the University of Hong Kong, completing a final year research project on luminescent Pt(II) complexes under the guidance of Prof. Vivian W.-W. Yam. He is currently a postdoctoral researcher in the group of Dr. Ho Yu Au-Yeung, working on the synthesis of stimuli-responsive catenane receptors.

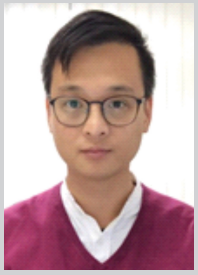

Ho Yu Au-Yeung is currently an Associate Professor at the University of Hong Kong. He obtained his BSc (First Class) and MPhil from The Chinese University of Hong Kong and a PhD from University of Cambridge, and was a Croucher Postdoctoral Fellow at UC Berkeley. His group is interested in supramolecular and mechanical bond chemistry. He is the recipient of the Croucher Innovation Award (2016), the Graeme Hanson Early Career Researcher Award (2016), Asian Core Program Lectureship Award (Taiwan, 2018) and HKU Outstanding Young Researcher Award (2020), and serves as a member of the Early Career Advisory Board of Chemical Reviews (2020-2022) and the Committee of Young Chemists of the Chinese Chemical Society (since 2019).

2. Rotaxanes from CBAAC

2.1. High-order [n]Rotaxanes and Rotaxane Dendrimers

Following the synthesis of the first [2]rotaxane via CBAAC as reported by Mock in 1989,[14] Tuncel and Steinke have exploited in the early 2000s the same strategy in the synthesis of CB[6]-containing rotaxanes and polyrotaxanes.[16] They initially investigated the possibility of preparing [3]- and [4]rotaxanes using mesitylene-based bis- and tris-azide/alkyne as precursors. Mesitylene groups were chosen because they are too bulky to fit inside the cavity of CB[6] and do not form inclusion complexes with the macrocycles, thereby allowing them to catalyze the 1,3-dipolar cycloaddition between the azide the alkyne functionalities. By reacting the mesitylene-based azide **1**, alkyne stopper **2** and CB[6] in 1:2:2 ratio in 6 M aqueous HCl, the corresponding [3]rotaxane **Rot-1** was obtained in 71% yield (Figure 3). Similarly, the analogous [4]rotaxane **Rot-2** was prepared in 75% yield via CBAAC by using the tris(propagylammonium) **3** with three equivalents of **4** and CB[6].

In a study reported by Keinan and co-workers, the sterically less bulky *p*-xylyl building block **5** was employed as one of the coupling partners in CBAAC rotaxane synthesis (Figure 4a).[17] Encapsulation of **5** by CB[6] at room temperature gave the pseudo[3]rotaxane **6** with one CB[6] bound to each of the ammonium terminal as the kinetic product, and subsequent CBAAC with **7** afforded the corresponding [3]rotaxane **Rot-3** in 95% yield. In contrast, heating a solution of CB[6] and **5** at 95 °C in 6 M aqueous HCl for 48 hours gave the corresponding pseudo[2]rotaxane **8** as the thermodynamic product, in which inclusion of the *p*-xylyl moiety strengthens the CB[6] binding with the two ammonium ions. As the CB[6] cavity has been occupied and unavailable for CBAAC, no rotaxane formation was observed upon addition of the bulky stopper **7**.

Following the successful synthesis of the [3]- and [4]rotaxanes, Tuncel and Steinke further extended their work to the preparation of polyrotaxanes using multi-functionalized mesitylene as monomers.[18] Reaction between the mesitylene derived bis-azidoethylammonium **9** and bis-propagylammonium **10** in the presence of two equivalents of CB[6] led to the linear mainchain polyrotaxanes **Rot-4** as colourless films with a number-average molecular weight (M_n) of up to 39,000 (Fig-

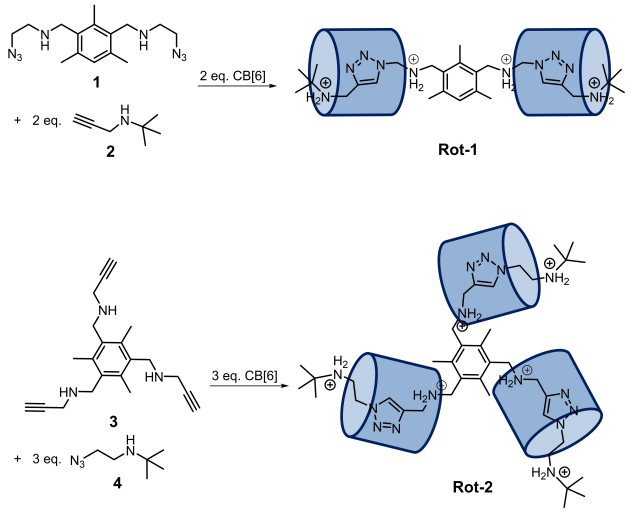

Figure 3. Tuncel's synthesis of [3]- and [4]rotaxanes via CBAAC.

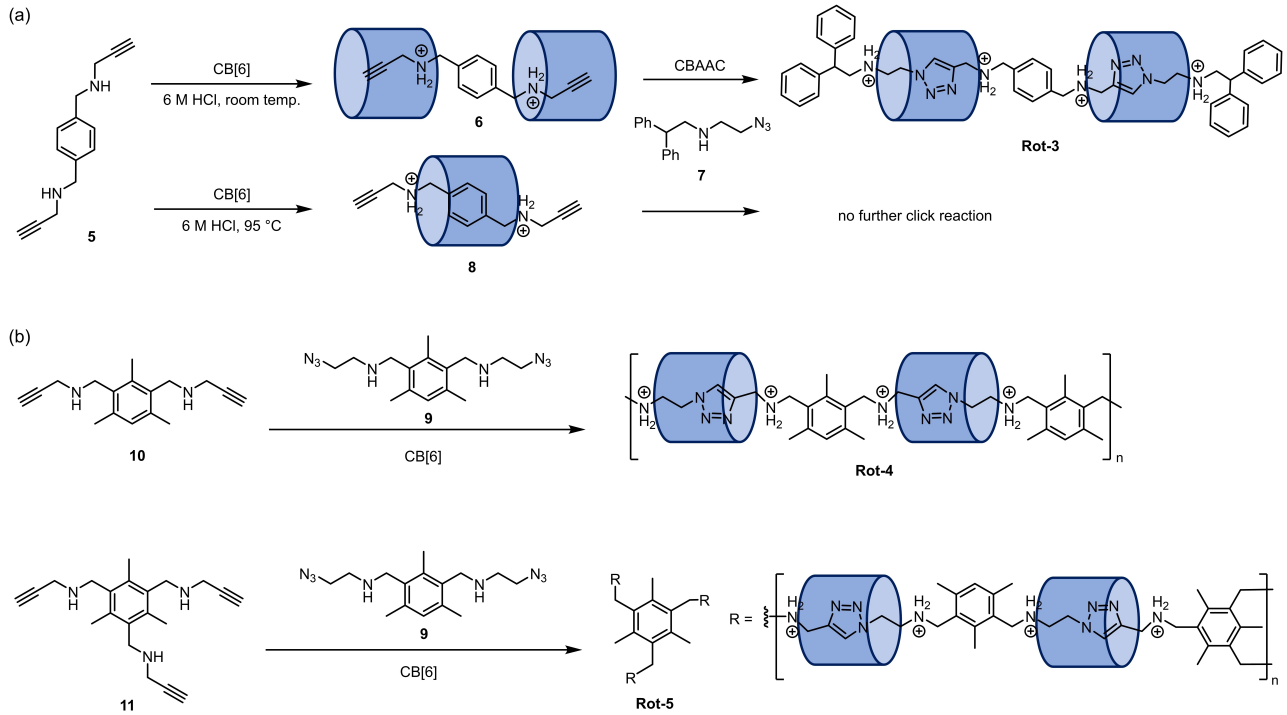

Figure 4. CBAAC mediated (a) [3]rotaxane synthesis by Keinan and (b) polyrotaxane synthesis by Tuncel.

ure 4b). ^{1}H NMR analysis of the polymers revealed that each triazole ring is encapsulated by a CB[6], and ring-dethreading is inhibited by the bulky mesitylene groups. By extending to the mesitylene-based tris-propagylammonium **11** and bis-azidoethylammonium **9** as the monomers in the CBAAC-mediated polymerization, the branched polyrotaxane **Rot-5** with M_n up to 34,000 was obtained.

In addition to [n]rotaxane and polyrotaxanes, CBAAC has also been employed in the synthesis of rotaxane-based dendrimers. In 2011, Lee and co-workers described the formation of [3]rotaxane dendrimers utilizing a convergent approach.[19] By reacting the pseudo[3]rotaxane derived from a *p*-xylyl core **6** and the azide-containing dendrons **12**–**14** in 5% aqueous HCl solution, the corresponding 1st, 2nd and 3rd generation rotaxane dendrimers **Rot-6**, **Rot-7** and **Rot-8** were obtained in 96% yields (Figure 5).

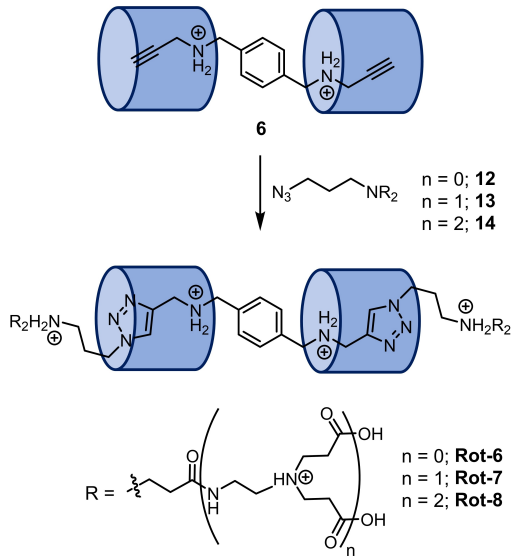

Figure 5. Lee's rotaxane dendrimer synthesis using CBAAC.

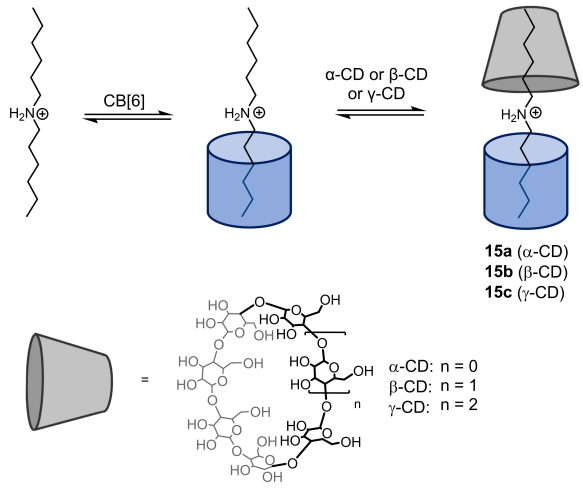

Figure 6. Formation of a ternary complex featuring cooperative binding between CB[6] and CDs on dihexylammonium.

2.2. Promoted CBAAC via Cooperative Capture

Apart from interacting with positively charged cations, the carbonyl portals of CB[6] can also form hydrogen bonds with hydrogen bond donors, and the cooperative binding between CB[6] and cyclodextrins (CDs) on a dialkylammonium guest has been first identified by Inoue and co-workers in 2006.[20] In their study, pseudo[3]rotaxanes **15a**–**c** have been formed from a CB[6]-dihexylammonium complex and a α-CD, β-CD or γ-CD, in which the two hexyl chains are separately encapsulated in the cavity of the two different macrocycles (Figure 6). Binding study by isothermal titration calorimetry showed an enhanced affinity of the α-CD and β-CD towards the hexyl chain in the CB[6]-complex than that of free hexylamine by 2-fold and 33-fold respectively, and the cooperative binding has been suggested to be due to the hydrogen bonding network between the two threaded macrocycles. The ^{1}H-^{1}H 2D ROESY spectrum of **15b** also revealed a close proximity between protons from the CB[6] and the secondary hydroxyl groups of the β-CD, suggesting that the cooperative interaction is stereoselective. By manipulating the interacting partners through the addition of β-CD/γ-CD, CB[6] and ammonium-based axles, reversible switching between a double-axle pseudo[3]rotaxane and a single-axle pseudo[4]rotaxane has also been reported by the same group.[21]

The cooperative CD-CB[6] interaction on organic ammonium guests can also promote CBAAC. In 2013, Stoddart and co-workers have reported the synthesis of the hetero[4]rotaxane **Rot-9** and **Rot-10** using **16**, **17**, CB[6] and β-CD/γ-CD in a 1:2:2:1 ratio (Figure 7).[22] Reaction rate of the CBAAC was found to be enhanced (>100-fold enhancement) and a quantitative rotaxane formation was observed after the reaction mixture has been heated at 80 °C for only one minute. In stark contrast, [3]rotaxane formation in the absence of the CD was found to be slow and incomplete even after the reaction mixture has been stirred at 80 °C for 2.5 hours and left standing at room temperature for one week. Furthermore, by heating a mixture of the ditolyl-based bis(alkyne) **17** and the ditolyl-based bis(azide) **19** in the presence of CB[6] and β-CD/γ-CD in water at 60 °C for one hour, polypseudorotaxanes **Rot-11** and **Rot-12** were afforded with a degree of polymerization of 15.8 and 7.5 respectively. This strategy of using additional components (i.e. CD) that cooperatively bind to the CB[6] to promote the CBAAC is described as cooperative capture.

Although the hydrogen bonds between the CDs and CB[6] in the above examples is suggested to play a major role in the cooperative binding and cooperative capture, contribution from the hydrophobic interactions between the CDs and hydrophobic moiety (e.g. the hexyl chain in Inoue's case and biphenyl unit in Stoddart's case) should be not ignored. In a recent example of [4]rotaxane synthesis from our laboratory, **Rot-13** and **Rot-14** which differ only by the interlocked β-CD and γ-CD were found to adopt very different co-conformations

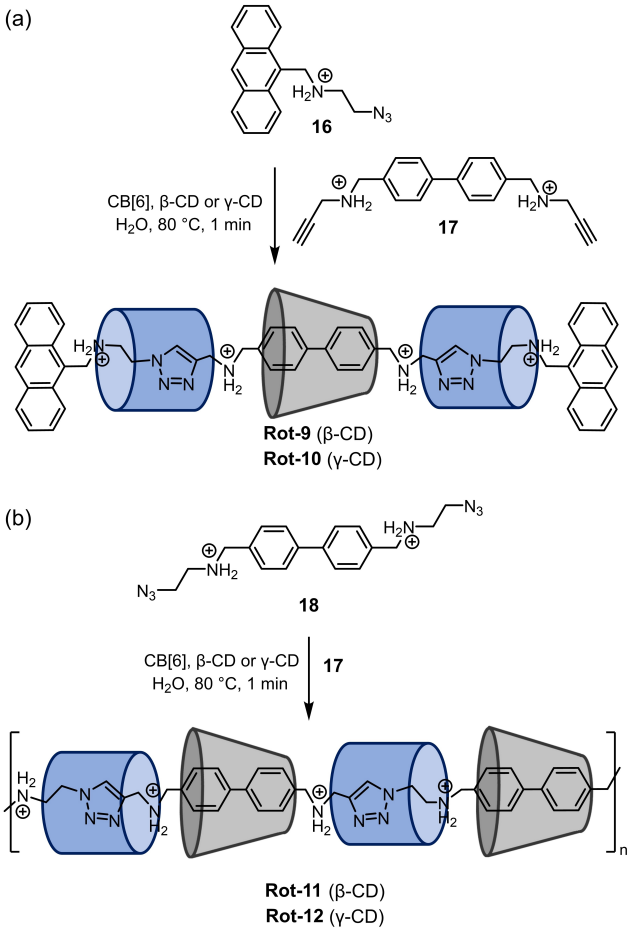

Figure 7. Stoddart's cooperative capture synthesis of (a) [4]rotaxanes and (b) poly[n]rotaxane.

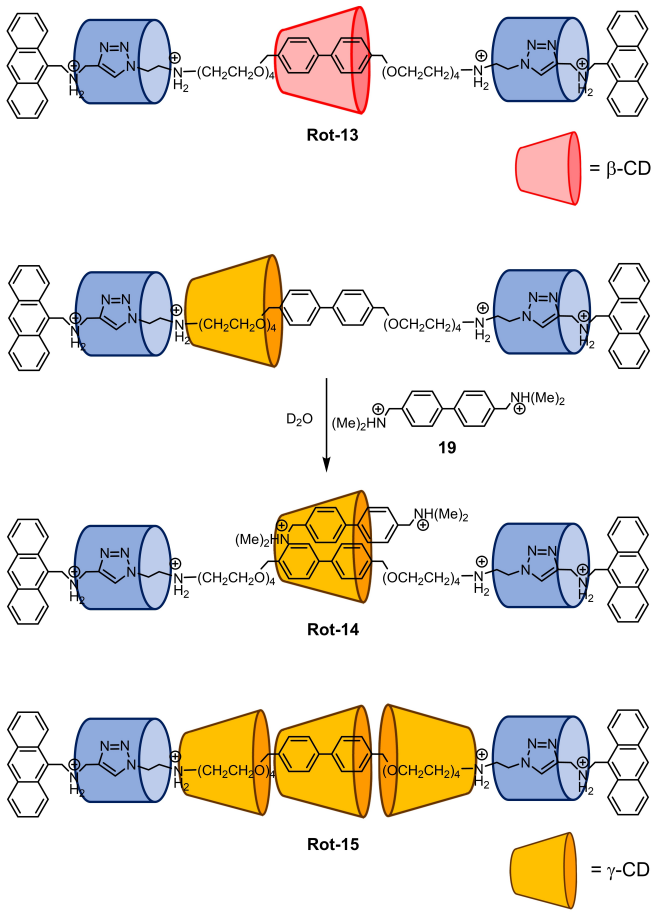

Figure 8. Hetero[4]rotaxanes **Rot-13** and **Rot-14**, and [6]rotaxane **Rot-15**.

(Figure 8).[23] In **Rot-13**, the β-CD was found to reside on the biphenyl station, whereas the γ-CD in **Rot-14** was found to be located next to the ammonium-bound CB[6] on the tetra(ethylene glycol) chain. The different co-conformations could be explained by the different stability of the two CDs at the biphenyl and hydrophilic tetra(ethylene glycol sites. While β-CD binds to biphenyl units with appreciable strength (log K_a ≈3), binding of a single biphenyl to the larger γ-CD is weaker with an inferior size complementarity. On the other hand,

although β-CD has been reported to show no binding to the hydrophilic poly(ethylene glycol), it has been reported that there is a weak but significant binding of γ-CD to poly(ethylene glycol), which is suggested to allow the macrocycle to further interact with the ammonium-bound CB[6] in the [4]rotaxane to give the observed co-conformation. In fact, shuttling of the interlocked γ-CD from the tetra(ethylene glycol) to the biphenyl station was observed upon addition of the aromatic guest **19** to a solution of **Rot-14** as a result of the formation of a stable heteroternary inclusion complex between the guest, the biphenyl on the axle and the γ-CD. Furthermore, additional γ-CD can be interlocked onto the axle by simply increasing the amount of γ-CD in the reaction, and the hetero[6]rotaxane **Rot-15** was obtained as a single stereoisomer, suggesting the weak interactions betwen the γ-CD and the hydrophilic tetra(ethylene glycol) chain may also be stereoselective and promote the CBAAC.[24]

To study and control the dynamics of the interlocked components, Yang and co-workers have prepared a series of hetero[4]rotaxanes featuring axles of different size and rigidity using interlocked γ-CD functionalized with a capping group for modulating the rotational kinetics.[25] For rotaxanes **Rot-16a** and **Rot-16b** consisting of the more flexible biphenyl-based axle, fast rotation was observed for both the phenyl- and naphthyl-capped γ-CD even at −20 °C (Figure 9). In contrast, when the more rigid naphthalene unit was incorporated in the axle of **Rot-17a** and **Rot-17b**, the phenyl-capped γ-CD in **Rot-17a** showed a fast macrocycle rotation, whereas a slow rotation was observed for the naphthyl-capped γ-CD in **Rot-17b** due to the increased rotational barrier because of the more significant steric hindrance between the two naphthyl groups of the interlocked axle and γ-CD.

In addition to CDs, Stoddart and co-workers have also extended the concept of cooperative capture by utilizing pillar[5]arene (PA[5]) in [n]rotaxane syntheses.[26] Compared to β-CD and γ-CD, PA[5] possesses more polarized hydrogen bond donors and are highly complementary to CB[6] in terms of their rim size. By combining PA[5], pseudo[2]rotaxane complex **24**

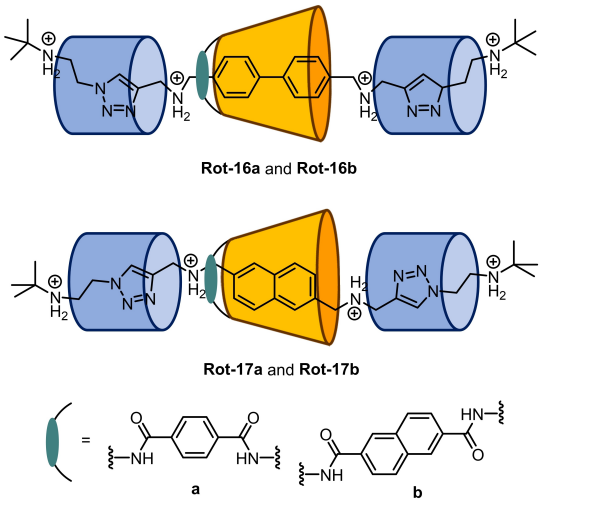

Figure 9. Yang's example of [4]rotaxanes with controllable rotational dynamics.

derived from CB[6] and stopper alkyne, and dialkylated bipyridiniums **20**–**23** with terminal azido groups, two [4]rotaxanes (**Rot-18** and **Rot-19**) and two [5]rotaxane (**Rot-20** and **Rot-21**) were synthesized in high yields within two hours at 55 °C in MeCN (Figure 10). Importantly, the addition of PA[5] not only accelerated the CBAAC on each side of the PA[5] portals, but also enabled the use of a broader range of substrates due to the ability of PA[5] to stabilize the otherwise unfavorable conformations of the azide and alkyne within the

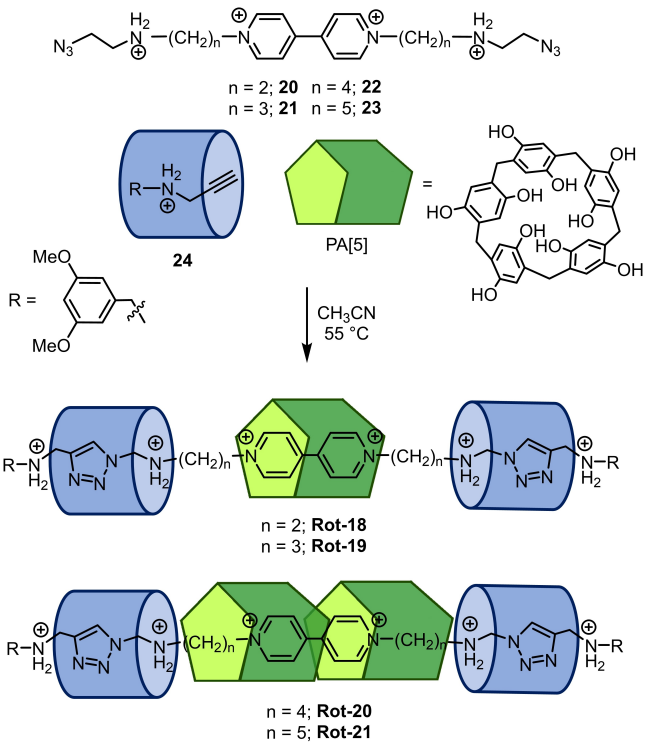

Figure 10. Stoddart's example of PA[5]-assisted CBAAC in rotaxane synthesis.

CB[6] cavity through the formation of inter-ring hydrogen bonds. Flipping of the hydroquinones in the PA[5] is inhibited as a result of the interlocking, and the PA[5] conformers are trapped in the [n]rotaxanes. Population of rotaxane isomer with the interlocked PA[5] in the thermodynamically most stable C_5-symmetric conformation was found to increase as the reaction temperature decreased from 55 °C to −10 °C. More recently, pillar[6]arene (PA[6]) has also been demonstrated to be capable of promoting CBAAC, and three hetero[4]rotaxanes were obtained by reacting the corresponding axle precursor, PA[6] and the CB[6] complex of the stopper.[27] In contrast to PA[5], oxygen-through-annulus rotation of the hydroquinones was still observed for the PA[6] in these rotaxanes because of the larger PA[6] cavity and their relatively weaker hydrogen bonds with CB[6].

3. Catenanes from CBAAC

3.1. High-Order [n]Catenane Synthesis

Catenanes are topologically non-trivial and composed of only interlocked macrocycles. Macrocycle formation is hence essential in catenane synthesis, and maintaining the preorganized components in a correct orientation during the covalent bond formation is therefore critical to the efficient synthesis of catenanes.[24] The precise control on the preorganization and macrocycle formation would become increasingly important as the number of interlocked macrocycles in the target [n]catenane increases, or otherwise complex mixtures of topological isomers containing different number and arrangement of interlocked macrocycles would be resulted.[29] In this regard, the strong ammonium-CB[6] binding and efficient CBAAC offer a good opportunity for the simultaneous interlocking and macrocycle formation to give complex [n]catenanes.

In 2018, our group has reported the aqueous synthesis of a series of [3]catenanes **Cat-1** using difunctionalized building blocks with terminal azidoethylammonium (**25a**–**h**) and propagylammonium groups (**26a**–**h**).[30] By varying the combinations of the click partners with different central units, a total of eleven [3]catenanes have been prepared in a simple one-step procedure using CBAAC in yields from 85% to 93% (Figure 11).

By using **25c**/**26c** and **25d**/**26g** which both contains biphenyl units for interlocking with β-CD as the click partners for CBAAC, we have also synthesized the first pair of catenane isomers that differs in the sequence of the interlocked macrocycles.[31] The [5]catenane **Cat-2** and **Cat-3**, featuring respectively a cyclic -ABAB- and -AABB- sequence of the interlocked CB[6] and β-CD, were obtained in 72% and 82% yield respectively through a one-step CBAAC (Figure 12). Of note, as the biphenyl units for β-CD binding in these building blocks are separated from the CB[6]-binding ammonium by a long tetra(ethylene) glycol chain, the CB[6] and β-CD are not close enough to result in cooperative capture, and indeed no significant enhancement in reaction rate was observed and formation of the [5]catenane was completed after overnight

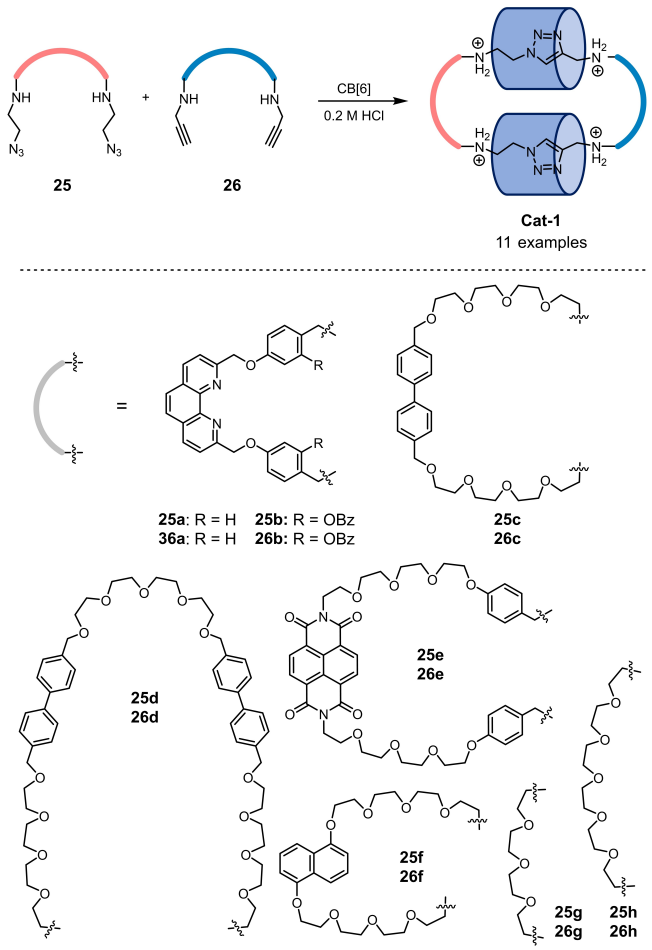

Figure 11. Synthesis of [3]catenanes by CBAAC.

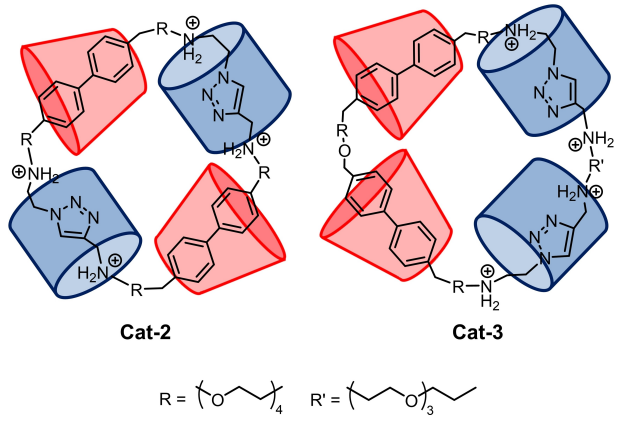

Figure 12. Isomeric radial [5]catenanes **Cat-2** and **Cat-3** with different sequence of CB[6] and β-CD threaded onto the central macrocycle. Only one possible β-CD orientation is shown.

heating of the reaction mixture at 80 °C. For the different strength of the CB[6]-bis(ammonium) binding (log $K_a \approx 5$–6) and hydrophobic β-CD binding to the biphenyl (log $K_a \approx 3$), the interlocked β-CDs are relatively more mobile whereas dynamics of the CB[6]s are relatively slow. Difference in the β-CD shuttling dynamics as a result of the interlocking sequence was revealed by variable temperature ^{1}H NMR. A higher coalescence temperature was found for **Cat-3** than the isomeric **Cat-2**, which could be explained by the mutually influencing motions of the two adjacent β-CDs in **Cat-3**. Moreover, while the hydrophobic interaction of β-CD is generally not considered to be pH sensitive, deprotonating the ammoniums resulted in the mobilization of the interlocked CB[6] and affects the dynamics of the β-CDs, as motions of the two differnet macrocycles are likely coupled in the [5]catenanes. More recently, similar [4]catenane isomers with one interlocked β-CD and central macrocycles with or without a CB[6] "speed bump" between two degenerated biphenyl stations have also been prepared and their dynamics were studied by detail NMR analysis.[32]

Apart from the radial [n]catenanes described above, CBAAC has also been used in the synthesis of branched [n]catenanes, in which a branched arrangement of the interlocked macrocycles is much less common than other radial or linear [n]catenanes. In 2016, our group has reported the one-pot synthesis of the branched [6]catenane **Cat-4** from building blocks **25 f** and **26 a** in the presence of a Cu^+ template in aqueous DMF.[33] For the good compatibility and orthogonality of the Cu^+-phenanthroline coordination and ammonium-CB[6] interactions, the [6]catenane was obtained in a good yield of 91% (Figure 13). By replacing the naphthalene unit with a biphenyl, as well as installing an additional benzyl group on the phenyl linker of the phenanthroline-derived building block, CBAAC between **25 c** and **26 b** in the presence of 10 eq. of β-CD gave the branched [8]catenane **Cat-5** in 72% yield, which is one of the highest order [n]catenane that has been isolated and characterized to date.[30] The benzyl group on the phenanthroline-derived building block was found critical to the [8]catenane synthesis, as the CBAAC under similar conditions using **25 c** and **26 a** that lacks the benzyl group was found to give the radial [5]catenane **Cat-6**, in which an extra β-CD was found to be interlocked at the phenyl linker in addition to the one at the biphenyl station. Model studies using related (pseudo)rotaxanes showed that β-CD can engage in a cooperative binding at the phenyl linker of **27 a** assisted by an ammonium-bound CB[6] ($K_1 = 1.8 \times 10^4$ M^{-1},and $K_2 = 8.2 \times 10^3$ M^{-1}), although the binding between β-CD and **26 a** at the phenyl linker is several order of magnitudes weaker ($K_a = 160$ M^{-1}).

4. Functional Rotaxanes from CBAAC

4.1. Inhibiting Radical Exchange and Controlling Stereochemistry of Photoisomerization

In 2011, Lucarini and co-workers reported the preparation of the first example of a CB[6]-containing [3]rotaxane interlocked on a paramagnetic axle with two nitroxide radicals at the stoppers.[35] The [3]rotaxane **Rot-22** was prepared in 75% yield from CBAAC by heating a mixture of the *p*-xylyl-derived building block **5** and the TEMPO-derived stopper **27** in the presence of CB[6] at 60 °C in 6 M aqueous HCl for 24 hours (Figure 14). The EPR spectrum of the [3]rotaxane **Rot-22** in water showed three lines as expected for a nitroxide radical,

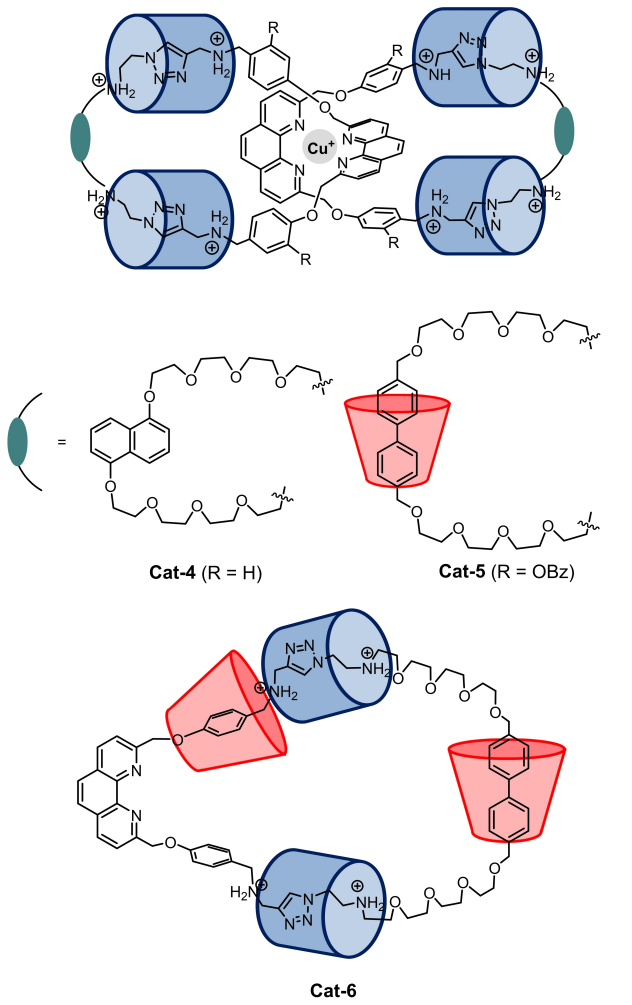

Figure 13. CBAAC synthesis of [5]-, [6]- and [8]catenanes. Only one stereoisomer of **Cat-5** and **Cat-6** is shown.

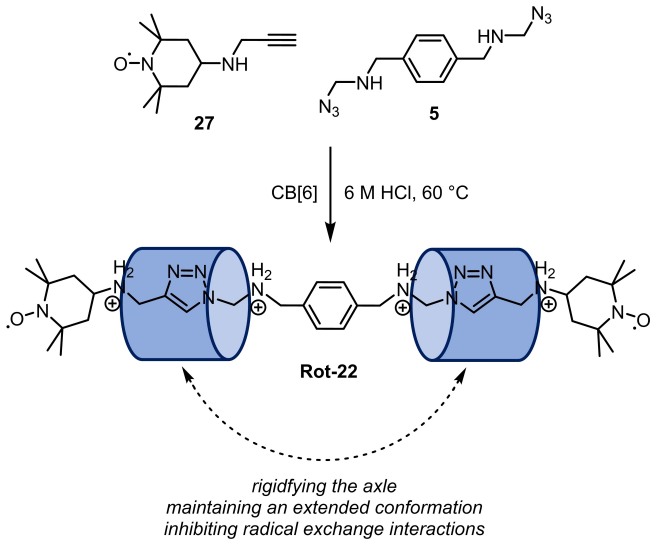

Figure 14. Lucarini's example of a paramagnetic rotaxane from CBAAC in which the interlocked CB[6]s inhibit the exchange interactions of the TEMPO radicals.

suggesting that the two TEMPO stoppers have no significant exchange interactions. On the other hand, the EPR spectrum of the axle that lack the interlocked CB[6] macrocycle showed broadened exchange peaks, suggesting the exchange interactions between the paramagnetic stoppers are inhibited by the presence of the bulky, interlocked CB[6] that keep the [3]rotaxane in an extended conformation.

In 2017, Yang and co-workers have exploited the highly confined chiral cavity of the interlocked γ-CD in rotaxanes for enantioselective (*Z,Z*)-1,3-cyclooctadiene photoisomerization.[36] In their study, the hetero[4]rotaxane **Rot-16a** containig a photosensitizing biphenyl axle encapsulated within the cavity of a functionalized γ-CD were prepared by cooperative capture (Figure 9). The rigid phenyl linker on the γ-CD primary face was designed to further restraint the chiral binding cavity of the γ-CD. ^{1}H NMR studies revealed an enhanced binding of (*Z,Z*)-1,3-cyclooctadiene of up to 10,330 M^{-1} in D_2O to the [4]rotaxane bearing a capped γ-CDs compared to the uncapped analogue. Photoisomerization of the encapsulated (*Z,Z*)-1,3-cyclooctadiene at 0.5 °C afforded the (*Z,E*)-1,3-cyclooctadiene isomer in up to 15.3% enantiomeric excess, which was the highest level of enantiodifferentiation reported at the time for supramolecular photochirogenesis (Figure 15).

4.2. pH-responsive molecular shuttles and nanovalves

The pH-dependent ion-dipole interactions between CB[6] and bis(ammonium) guests render the MIMs prepared via CBAAC suitable to function as pH-responsive switches. For example, Tuncel has reported the CBAAC synthesis of the water-soluble [5]rotaxane **Rot-23**, with one CB[6] threaded onto each arm of a tetraphenylporphyrin-based axle (Figure 16), and its pH-dependent ring-shuttling behavior was studied using ^{1}H NMR spectroscopy in D_2O.[37] Under acidic condition (pH = 3.5), both the *tert*-butyl amine and porphyrin-benzylamine groups are protonated, and all the CB[6] rings were observed to reside

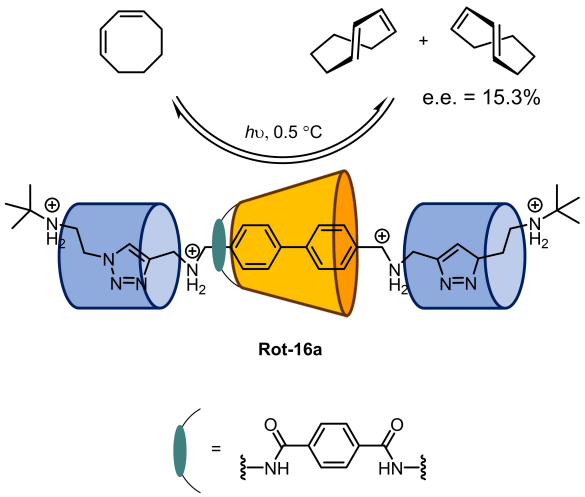

Figure 15. Enantioselective photoisomerization of (*Z,Z*)-1,3-cyclooctadiene inside the cavity of the photosensistizer **Rot-16a** resulted in an enantomeric excess (e.e.) of 15.3%.

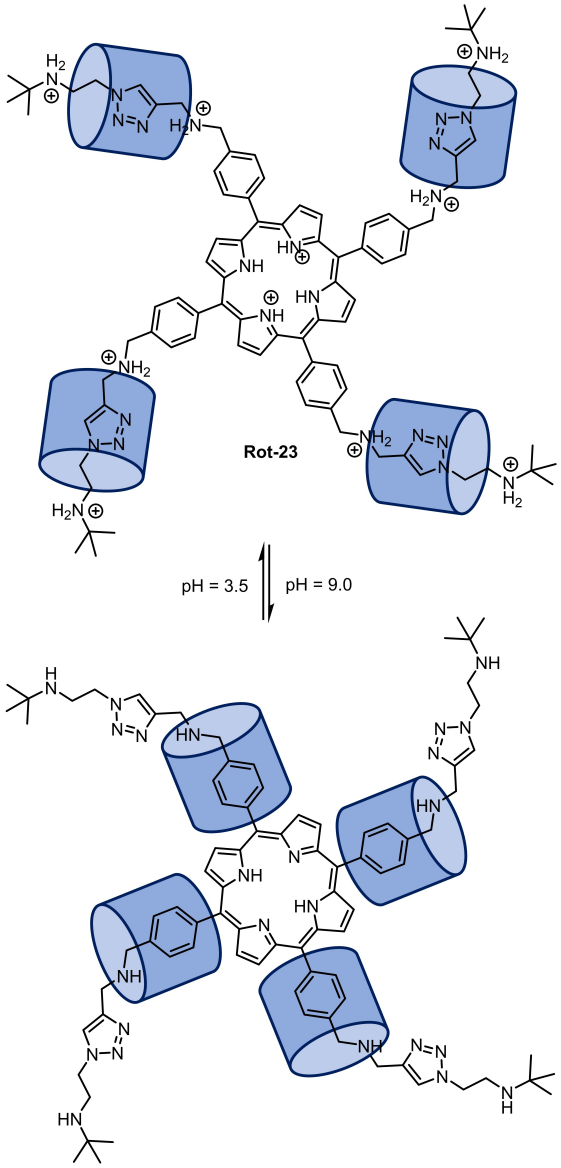

Figure 16. Tuncel's example of a pH-responsive [5]rotaxane obtained from CBAAC.

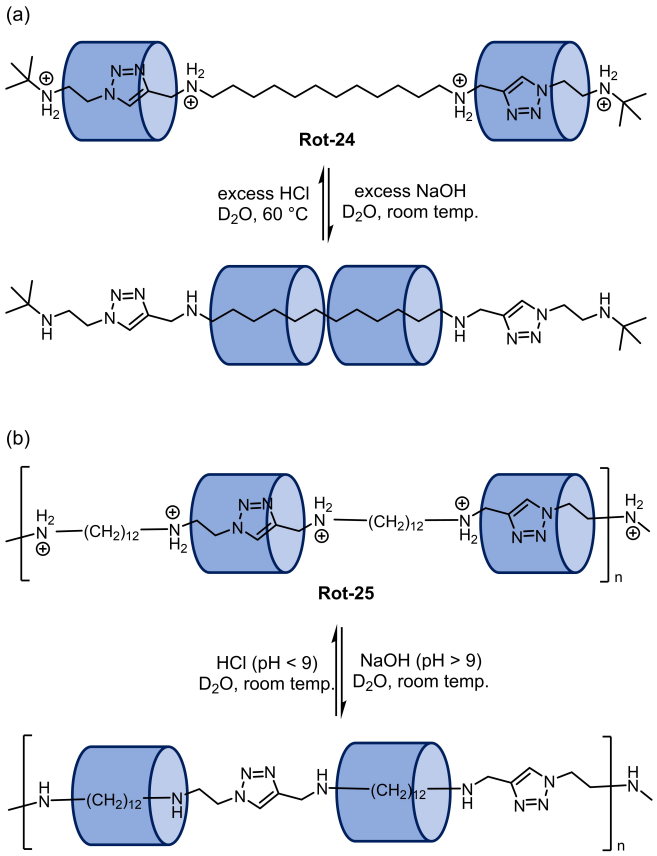

Figure 17. Co-conformational switching induced by pH in a (a) [3]rotaxane and (b) polypseudorotaxane.

over the triazole bis(ammonium) stations that are stabilized by hydrophobic and ion-dipole interactions. Upon increasing the pH from 3.5 to 9.0 via the addition of triethylamine, the ammonium groups were deprotonated, conceivably disrupting the ion-dipole interactions and causing the CB[6]s to shuttle to the more hydrophobic benzyl stations. Reprotonation of the porphyrin-based switch via the addition of aqueous HCl to pH 3.5 restores the ion-dipole interactions and allows the CB[6]s to shuttle back to the triazole sites.

Tuncel and co-workers have also investigated the pH-induced shuttling behaviors of the [3]rotaxane **Rot-24** consisting of two types of recognition sites, namely diaminotriazole and dodecamethylene groups (Figure 17a).[38] Initially, the two CB[6] rings form a stable inclusion complex with the protonated diaminotriazole stations as indicated by ^{1}H NMR analysis. Upon deprotonation of the ammonium groups via the addition of NaOH, the ion-dipole interactions between the CB[6] and the ammonium groups are disrupted and the two rings shuttle towards the central hydrophobic dodecyl station as a result of the more favorable hydrophobic interactions involving the long dodecyl chain, which is long enough to accommodate the two CB[6]s without significant steric repulsion. Interestingly, slow ring-shuttling was observed upon reprotonation of the axle, with only about half of the CB[6] rings shuttled back to the initial triazole stations after stirring at room temperature for 18 days. Kinetic analysis using Eyring plot revealed an activation barrier of ~100 kJ/mol for the back shuttling which is attributed to the relatively stable inclusion of the dodecyl chain in the CB[6] cavity. This ring-shuttling process can be accelerated by heating the rotaxane solution at 60 °C for three days.

The concept of molecular switches based on triazole and dodecyl station has also been extended by Tuncel in the synthesis of the pH-responive polypseudorotaxane **Rot-25** (Figure 17b).[39] By combining stoichiometric amount of dodecyl bis(azidoethylammonium) and dodecyl bis(propagylammonium) with two equivalents of CB[6], the corresponding polypseudorotaxane was obtained via the aforementioned catalytic self-threading process mediated by CBAAC (Figure 4). ^{1}H NMR analysis of the polymer sample revealed a M_n of 20,800. Addition of a base led to the shutting of the CB[6]s from the triazole to the dodecyl stations, with one CB[6]

occupying one dodecyl group. Upon raising the pH of the polymer solution from 5 to 9 to 11, the percentage of occupied dodecyl stations in the polymer chains was found to increase from 0% to 50% to 95%. In contrast to the [3]rotaxane described before, back shuttling of the CB[6] to the triazole stations was observed five minutes after the addition of aqueous HCl.

The pH-dependent CB[6] binding property has also been exploited by Stoddart and co-workers in the preparation of pH-responsive supramolecular nanovalves that can operate under aqueous conditions.[40] The nanovalves **28** are prepared by CBAAC between dye-loaded alkyne-functionalized mesoporous silica gel nanoparticles and 2-azidoethylammonium, which installed a layer of pseudo[2]rotaxanes on the nanoparticle surface (Figure 18). The comparable size of CB[6] (diameter = 1.4 nm) to the nanopores (diameter = *ca.* 2 nm) allowed the CB[6] to efficiently block the nanopores and prevent the encapsulated dye from leaking out. Upon raising the pH of a solution of **28**, emission was found to slowly increases over time, suggesting the nanovalves are opened upon ammonium deprotonation and subsequent CB[6] dethreading that release the fluorescent dye from the nanoparticles. Efficiency of the nanovalves is dependent on the length of the linker between CB[6] and the nanoparticle surface. While detectable dye leakage was observed prior to base-induced nanovalve-opening in **28a**, replacing the propyl linkers with shorter methyl linkers between the silicon and ammonium groups places the CB[6] caps closer to the nanopores, thereby inhibiting leakage whilst retaining the base-induced nanovalve-opening property.

4.3. Light responsive and luminescent rotaxanes

Rotaxanes synthesized via CBAAC have also been employed as potential photosensitizers for photodynamic therapy. In 2019, Tuncel and co-workers investigated the photosensitizing ability of the previously reported porphyrin-based [5]rotaxane **Rot-23** synthesized via CBAAC (Figure 16).[41] In dark, the photosensitizer exhibited negligible cytotoxicity towards bacterial cells (i.e., *E. coli* and *B. subtilis*) and the mammalian breast cancer cell line MCF7. Upon white light illumination, **Rot-23** can generate reactive oxygen species (ROS) and became photocytotoxic at a concentration as low as 2 μM under relatively low luminous flux (22 mW/cm^2) and short exposure period (1 minute). Compared to the control tetra-alkynyl porphyrin axle precursor, **Rot-23** demonstrated superior aqueous solubility that is attributed to the inhibited π-π stacking of the porphyrin cores due to the bulky CB[6]. Moreover, the control non-interlocked porphyrin axle was found to exhibit dark cytotoxicity due to the presence of cationic ammonium groups, which were disguised in the rotaxane-based photosensitizer by the CB[6] binding.

Later, by utilizing the photosensitizing behavior of the porphyrin-based rotaxanes, the same group has developed a strategy to synthesize a thin-film of polyrotaxane network (Figure 19).[42] Similar to the aforementioned [5]rotaxane, the polyrotaxane thin film (**Rot-26**) is capable of generating ROS and killing both Gram-positive (*E. coli*) and Gram-negative (*B. subtilis*) bacteria under white light illumination, and its antimicrobial property can be efficiently switched off in the dark.

By exploiting cooperative capture condition, Stoddart and co-workers have recently reported the preparation of hetero[4]rotaxane **Rot-27** featuring a tunable solid-state emission for supramolecular encryption.[43] Fluorescence study on the hetero[4]rotaxane revealed an almost quantitative Förster resonance energy transfer (FRET) efficiency from the pyrene donor (λ_{ex} = 340 nm) in the stopper to the diazaperopyrenium

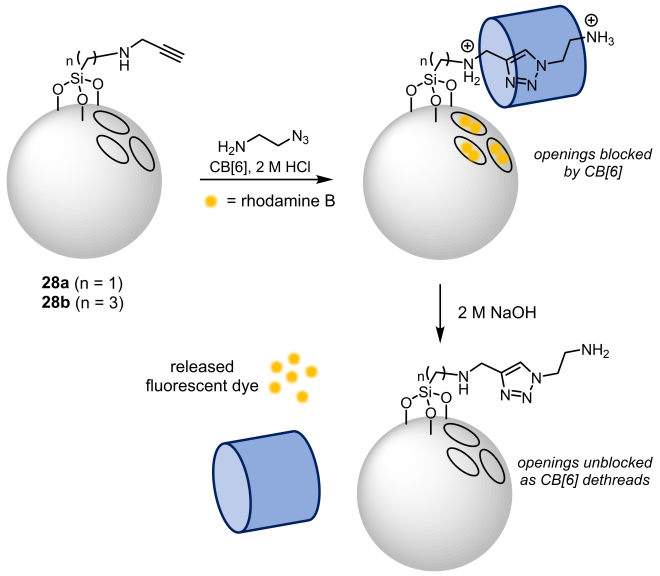

Figure 18. Nanovalves decorated by a pseudo[2]rotaxane via CBAAC control the release of a fluorescent load.

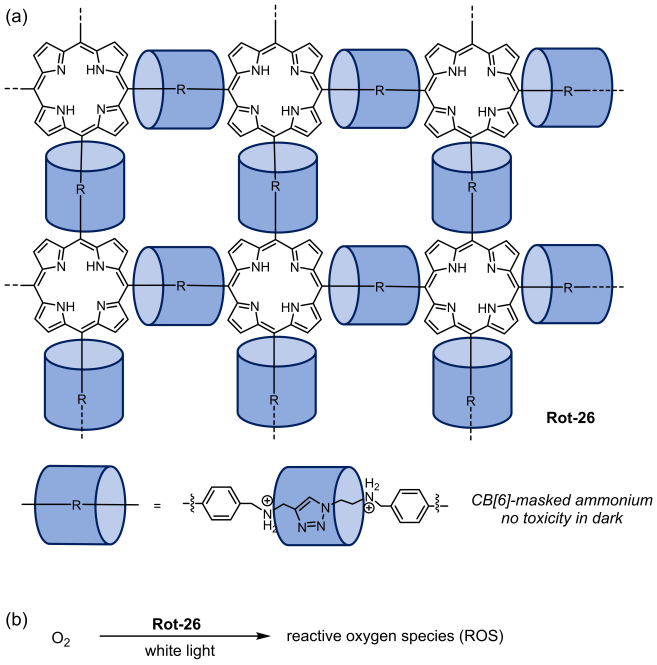

Figure 19. (a) Strcuture of the rotaxane-based thin file **Rot-26**, and (b) reactive oxygen species (ROS) generation mediated by **Rot-26** upon light sensitization.

acceptor in the axle (λ_{em} = 510 nm) (Figure 20). The good FRET efficiency is attributed to i) the close proximity between the donor and acceptor units (ca. 1.2 Å), ii) the limited conformational flexibility due to the presence of the interlocked macrocycles that reduces the non-radiative decay, and iii) the inhibited aggregation-induced quenching as a result of mechanical protection in the rotaxane. Emissions of the rotaxane in both the aqueous solution and solid sample were also found to be dependent on both the rotaxane concentration and the presence of external stimuli. The rotaxane was found to aggregate at high concentration, and this was manifested in the decrease of the sharp diazaperopyrenium emission at 510 nm and the emergence of a broad and featureless band at 610 nm originated from the diazaperopyrenium/pyrene exciplex. Addition of γ-CD that binds to the pyrene termini led to a decreased extend of the aggregation, and the binding can be reversed by introducing a competitive guest (e.g. 2-adamantylamine chloride). Hence, colour of the rotaxane solid can be fine-tuned over a wide emission spectrum by *ca.* 100 nm via adjusting the concentration of rotaxane and/or adding γ-CD and a competitive guest. The use of the tunable emission from the [4]rotaxane was further demonstrated as a security ink for supramolecular encryption.

Yang and co-workers have reported in 2019 a series of water-soluble hetero[4]rotaxanes displaying room-temperature phosphorescence (RTP) for selective tryptophan detection.[44] The [4]rotaxanes **Rot-28** and **Rot-29**, showing a RTP quantum yield of 2.67% and 2.90% respectively, were prepared by using the mono- or bis-iodinated γ-CDs via cooperative capture (Figure 21). In fact, RTP is rarely observed in metal-free organic chromophore and the unusual RTP in these [4]rotaxanes is suggested to be a combined result of i) the heavy iodine atoms on the γ-CDs that promote intersystem crossing, and ii) the protective environment of the naphthalene chromophore inside the γ-CD cavity that significantly reduces collision with solvent molecules and non-radiative decay. Phosphorescence study revealed the RTP of the rotaxanes can be selectively quenched by tryptophan in pH 7.0 phosphate buffer, and the quenching is selective against other common amino acids. Isothermal titration calorimetry revealed an association constant of 610 M^{-1} for the binding between tryptophan and **Rot-29**, which is suggested to be driven by a combination of hydrophobic effect and π–π stacking interactions between the indole group of the amino acid and the naphthalene moiety in the rotaxane axle.

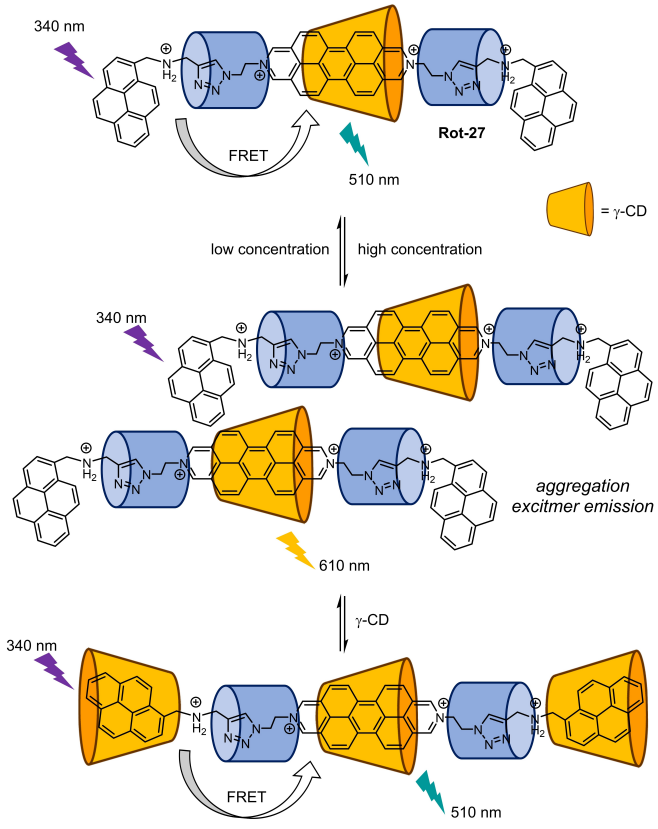

Figure 20. Hetero[4]rotaxane **Rot-27** featuring multistates emission controllable by concentration and external guests.

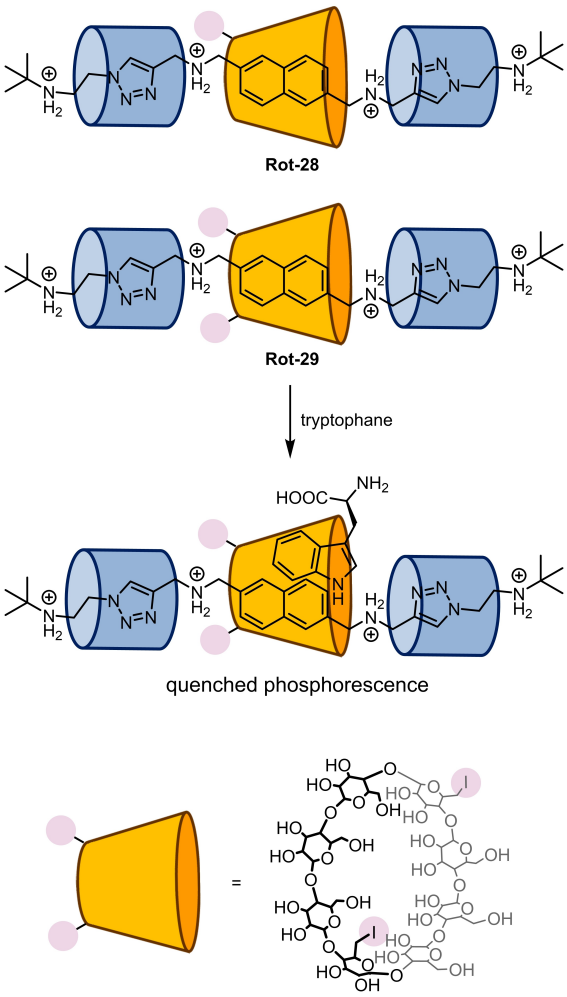

Figure 21. Hetero[4]rotaxanes **Rot-28** and **Rot-29** that displays room temperature phosphorescence, and that of the latter can be selectively quenched by tryptophane binding to the central cavity of the interlocked CD.

4.4. Rotaxanes from CBAAC for Biological Applications

In 2016, Francis and co-workers have reported the strategic use of a CB[6]-containing rotaxane **Rot-30** obtained from CBAAC for triggering the encapsulation of ^{129}Xe and controlling the ^{129}Xe signal in hyperCEST NMR upon external stimulation.[45] Hyperpolarized ^{129}Xe NMR coupled with chemical exchange saturation transfer (CEST) between free and bound Xe (^{129}Xe hyperCEST NMR) is a powerful and sensitive technique for biomarker detection, and one approach for the selective formation of host-bound ^{129}Xe signal at the region of interest is to induce the release of a pre-bound host for ^{129}Xe (e.g. CB[6]) that is occupied by another guest. In their work, a [2]rotaxane (**Rot-30**) was prepared by CBAAC (Figure 22). As a result of the axle-threading, the CB[6] cavity is occupied and its binding to ^{129}Xe was inhibited with a fully suppressed CB[6]-bound ^{129}Xe hyperCEST NMR signal. Upon the addition of a base (e.g. LiOH) that hydrolyzes the ester linkage and deprotonates the ammoniums in the axle, the CB[6] was released and ^{129}Xe binding was switched on, leading to a sharp signal in ^{129}Xe hyperCEST NMR. Later, the same group introduced a protease-cleavable peptide sequence in the axle of a similar rotaxane system (**Rot-31**) for detecting enzymatic activity using ^{129}Xe hyperCEST NMR.[46]

In 2017, Francis and co-workers have developed a strategy to prepare complex protein-based bioconjugates (**Rot-32**) utilizing CBAAC.[47] In their work, piperidine-based azidoethylamine was appended onto a protein to give **29**, and propagyl ammonium group was installed onto different substrates (i.e., polymer, DNA, peptide and drug) as the CBAAC partners. Under the optimized conditions, a range of bioconjugates including protein-polymer, protein-peptide, protein-DNA and protein-drug conjugates featuring a rotaxane structure were synthesized (Figure 23). Interestingly, rate enhancement of the CBAAC and almost quantitative conversion were observed during the preparation of the protein-drug conjugates between tobacco mosaic virus capsid protein (TMV) and doxorubicin (DOX), which is attributed to the formation of hydrogen bonds between DOX and CB[6] similar to the cooperative capture in the presence of CDs or PAs.

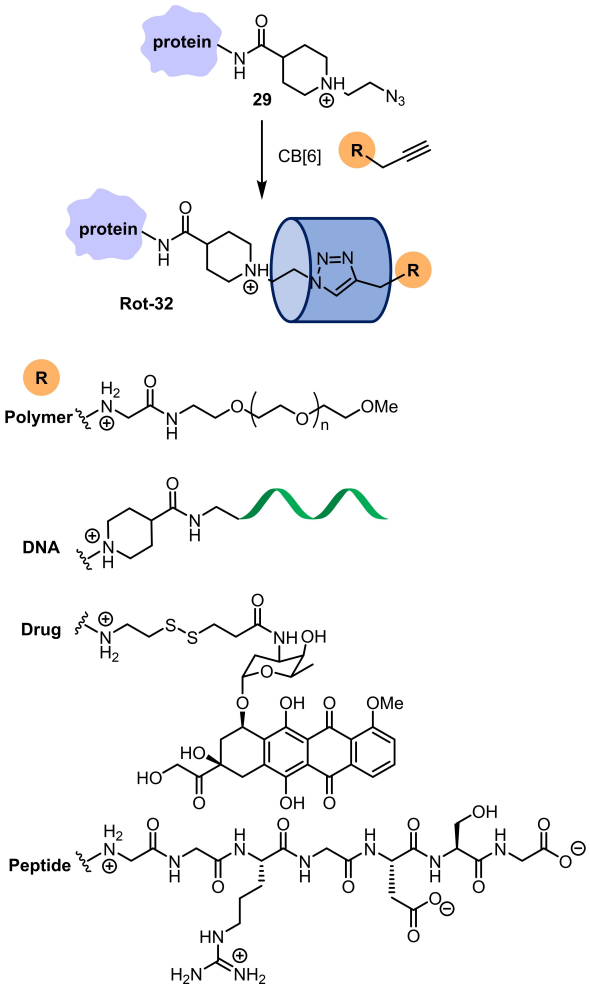

Figure 22. (a) Structures of cleavable [2]rotaxanes that can be activated by a base or an enzyme, and (b) the base-triggered hydrolysis of **Rot-30** that releases the interlocked CB[6] for ^{129}Xe hyperCEST NMR. [Dear Editor Team, please swap the figures in Figure 22 and Figure 23, but keep the same figure captions]

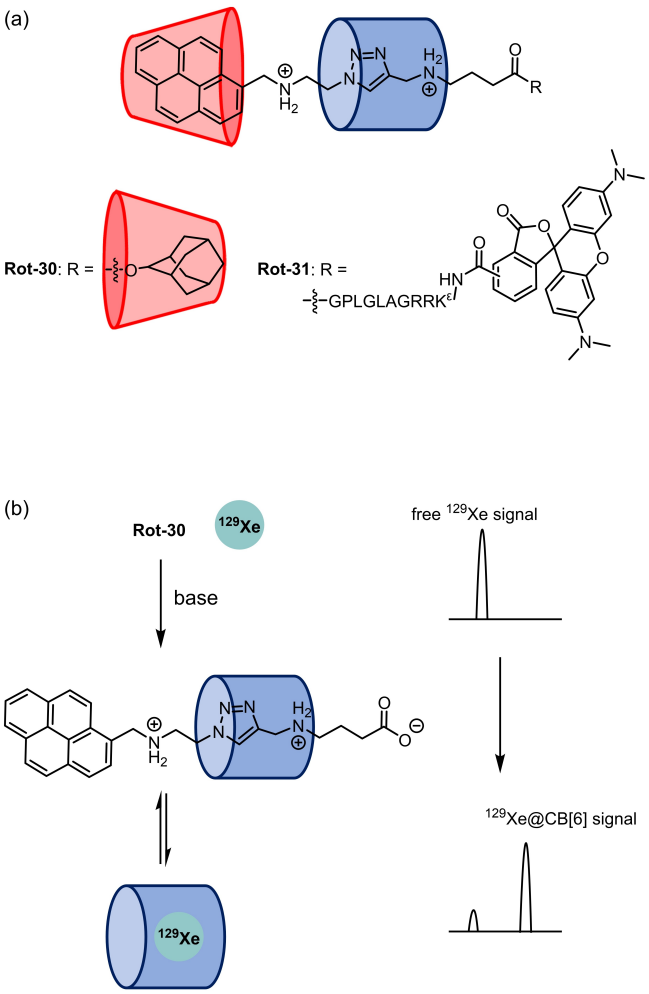

Figure 23. Protein-based bioconjugation utilizing CBAAC. [Dear Editor Team, please swap the figures in Figure 22 and Figure 23, but keep the same figure captions]

CBAAC under a cooperative capture condition has also been exploited by Holland and co-workers in the preparation of a rotaxane-based probe for *in vivo* imaging of cancer biomarkers.[48] In their work, a metal complex derived from the radioactive ^{89}Zr was employed as a bulky stopper in **Rot-33**, which is also linked via the β-CD by a photo-induced ligation to a monoclonal antibody that binds to human epidermal growth-factor receptor 2, thus enabling tumour radiolabelling and biodistribution analysis of the pharmacokinetic profiles via positron emission tomography (PET) imaging (Figure 24). Other radioactive metal labels (e.g. ^{68}Ga), protein- or peptide-based drugs, and fluorophores can also be incorporated similarly into the rotaxane architecture to give a variety of imaging probes. Very recently, Holland co-workers performed a detailed investigation into the synthetic scope of cooperative capture synthesis of hetero[4]rotaxanes, by using β-CDs appended with different reactive handles (e.g., azides, carboxylates, amines) that can potentially be further functionalized with biologically active vectors.[49] To provide further insights into the mechanism of cooperative capture synthesis, kinetic analysis and DFT calculations were performed to elucidate the reaction pathways, which revealed that the second CBAAC click reaction was the rate-determining step in hetero[4]rotaxane synthesis. The role of β-CDs in accelerating the CBAAC reaction rate was also studied by DFT calculations and natural bond orbital (NBO) analysis.

5. Conclusions

The unique capability of CB[6] to simultaneously i) catalyze the click reactions between azide and alkyne in CBAAC and ii) act as the macrocyclic component in the resulting MIMs distinguishes it from the rest of macrocyclic hosts. Seminal study by Mock revealed that the catalytic behavior of CB[6] is linked to its highly complementary cavity size to not only form ternary complexes with both alkyne and azide, but also impose strain to both bound substrates.

Conceptually, CBAAC is similar to active template strategy, in which a macrocycle accelerates the axle or macrocycle formation through its cavity to capture the mechanically interlocked structures. Both transition metal mediated (e.g. Cu(I), Ni(II), Pd(II))[50] and, more recently, metal-free[51] active template systems have been developed to enable the preparation of MIMs predominantly in organic, non-aqueous solvents. In contrast, the employment of CB[6] macrocycle in triazole formation allows the reaction to proceed smoothly in aqueous environment and be essentially metal-free, enabling access to myriad of interlocked molecules with various functionality for diverse applications. The ability of CB[6] to form hydrogen bonds with appropriate macrocycles (i.e., CDs, PAs) has been exploited in cooperative capture, which not only further accelerates CBAAC, but also widens the substrate scope and endows richer dynamic properties to the resulting high-order MIMs. The versatility of CBAAC also allows the fabrication of rotaxanes and catenanes that are stimuli-responsive, or suitable for biologically related applications.[52] Since the discovery of CBAAC four decades ago, the reaction has slowly progressed from assisting the preparation of aesthetically pleasing rotaxanes and catenanes, to now an invaluable synthetic tool that furnishes the mechanical bonds in interlocked architectures possessing practical real-life applications. For its adaptability and simplicity, CBAAC is envisioned to continue as the reaction of choice in the future to prepare highly sophisticated and functional mechanically interlocked systems.

Acknowledgements

We acknowledge the CAS-Croucher Funding Scheme for Joint Laboratories, a Collaborative Research Grant (C7075-21G) and a General Research Fund (17313222) from the Research Grant Council of Hong Kong for supporting our work.

Conflict of Interests

The authors declare no conflict of interest.

Data Availability Statement

Data sharing is not applicable to this article as no new data were created or analyzed in this study.

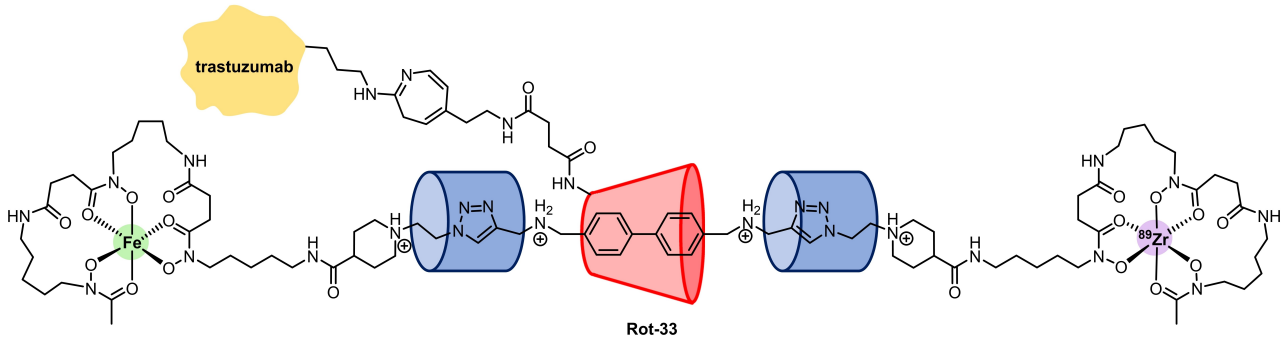

Figure 24. Holland's radiolabelled rotaxane synthesized by CBAAC.

Keywords: cucurbituril · click chemistry · catenane · mechanical interlocking · rotaxane

[1] C. J. Bruns, J. F. Stoddart, *The nature of the mechanical bond: from molecules to machines*. John Wiley & Sons, Inc., Hoboken, New Jersey, **2017**.
[2] a) J. E. M. Lewis, M. Galli, S. M. Goldup, *Chem. Commun.* **2017**, *53*, 298; b) N. H. Evans, *Chem. Eur. J.* **2018**, *24*, 3101; c) K. M. Bąk, K. Porfyrakis, J. J. Davis, P. D. Beer, *Mater. Chem. Front.* **2020**, *4*, 1052.
[3] a) M. J. Langton, P. D. Beer, *Acc. Chem. Res.* **2014**, *47*, 1935; b) M. J. Chmielewski, J. J. Davis, P. D. Beer, *Org. Biomol. Chem.* **2009**, *7*, 415; c) H. M. Tay, P. Beer, *Org. Biomol. Chem.* **2021**, *19*, 4652.
[4] a) M. W. Ambrogio, C. R. Thomas, Y.-L. Zhao, J. I. Zink, J. F. Stoddart, *Acc. Chem. Res.* **2011**, *44*, 903; b) C. Moon, Y. M. Kwon, W. K. Lee, Y. J. Park, V. C. Yang, *J. Controlled Release* **2007**, *124*, 43; c) A. Fernandes, A. Viterisi, F. Coutrot, S. Potok, D. A. Leigh, V. Aucagne, S. Papot, *Angew. Chem. Int. Ed.* **2009**, *48*, 6443; d) A. Fernandes, A. Viterisi, V. Aucagne, D. A. Leigh, S. Papot, *Chem. Commun.* **2012**, *48*, 2083; e) Barat, T. Legigan, I. Tranoy-Opalinski, B. Renoux, E. Péraudeau, J. Clarhaut, P. Poinot, A. E. Fernandes, V. Aucagne, D. A. Leigh, S. Papot, *Chem. Sci.* **2015**, *6*, 2608; f) T. Kench, P. A. Summers, M. K. Kuimova, J. E. M. Lewis, R. Vilar, *Angew. Chem. Int. Ed.* **2021**, *60*, 10928.
[5] a) D. A. Leigh, V. Marcos, M. R. Wilson, *ACS Catal.* **2014**, *4*, 4490; b) C. Kwamen, J. Niemeyer, *Chem. Eur. J.* **2021**, *27*, 175; c) R. Mitra, H. Zhu, S. Grimme, J. Niemeyer, *Angew. Chem. Int. Ed.* **2017**, *56*, 11456; d) L. Zhu, J. Li, J. Yang, H. Y. Au-Yeung, *Chem. Sci.* **2020**, *11*, 13008; e) Y. Jiao, L. Đorđević, H. Mao, R. M. Young, T. Jaynes, H. Chen, Y. Qiu, K. Cai, L. Zhang, X.-Y. Chen, Y. Feng, M. R. Wasielewski, S. I. Stupp, J. F. Stoddart, *J. Am. Chem. Soc.* **2021**, *143*, 8000; f) A. Bessaguet, Q. Blancart-Remaury, P. Poinot, I. Opalinski, S. Papot, *Angew. Chem. Int. Ed.* **2023**, *62*, e202216787; g) X. Mo, Y. Deng, S. K.-M. Lai, X. Gao, H.-L. Yu, K.-H. Low, H.-L. Wu, H. Y. Au-Yeung, E. C. M. Tse, *J. Am. Chem. Soc.* **2023**, *145*, 6087; h) A. W. Heard, J. M. Suárez, S. M. Goldup, *Nat. Chem. Rev.* **2022**, *6*, 182.
[6] a) G. De Bo, *Chem. Sci.* **2018**, *9*, 15; b) N. H. Pérez, J. E. M. Lewis, *Org. Biomol. Chem.* **2020**, *18*, 6757; c) L. Chen, X. Sheng, G. Li, F. Huang, *Chem. Soc. Rev.* **2022**, *51*, 7046; d) L. Wang, L. Cheng, G. Li, K. Liu, Z. Zhang, P. Li, S. Dong, W. Yu, F. Huang, X. Yan, *J. Am. Chem. Soc.* **2020**, *142*, 2051; e) J. Zhao, Z. Zhang, L. Cheng, R. Bai, D. Zhao, Y. Wang, W. Yu, X. Yan, *J. Am. Chem. Soc.* **2021**, *144*, 872; f) R. Stevenson, M. Zhang, G. De Bo, *Polym. Chem.* **2020**, *11*, 2864; g) M. Zhang, G. De Bo, *J. Am. Chem. Soc.* **2020**, *142*, 5029; h) R. Sandoval-Torrientes, T. R. Carr, G. De Bo, *Macromol. Rapid Commun.* **2021**, *42*, 2000447.
[7] a) C. W. Tornøe, C. Christensen, M. Meldal, *J. Org. Chem.* **2002**, *67*, 3057; b) V. V. Rostovtsev, L. G. Green, V. V. Fokin, B. K. Sharpless, *Angew. Chem. Int. Ed.* **2002**, *41*, 2596.
[8] a) O. Š. Miljanić, W. R. Dichtel, I. Aprahamian, R. D. Rohde, H. D. Agnew, J. R. Heath, J. F. Stoddart, *QSAR Comb. Sci.* **2007**, *26*, 1165; b) K. D. Hännia, D. A. Leigh, *Chem. Soc. Rev.* **2010**, *39*, 1240; c) B. T. Shahraki, S. Maghsoudi, Y. Fatahi, N. Rabiee, S. Bahadorikhalili, R. Dinarvand, M. Bagherzadeh, F. Verpoort, *Coord. Chem. Rev.* **2020**, *423*, 213484.
[9] a) W. L. Mock, N. Y. Shih, *J. Org. Chem.* **1983**, *48*, 3618; b) K. Kim, *Chem. Soc. Rev.* **2002**, *31*, 96; c) J. W. Lee, S. Samal, N. Selvapalam, H.-J. Kim, K. Kim, *Acc. Chem. Res.* **2003**, *36*, 621; d) J. Lagona, P. Mukhopadhyay, S. Chakrabarti, L. Isaacs, *Angew. Chem. Int. Ed.* **2005**, *44*, 4844; e) K. Kim, N. Selvapalam, Y. H. Ko, K. M. Park, D. Kim, J. Kim, *Chem. Soc. Rev.* **2007**, *36*, 267; f) L. Isaacs, *Acc. Chem. Res.* **2014**, *47*, 2052; g) S. J. Barrow, S. Kasera, M. J. Rowland, J. del Barrio, O. A. Scherman, *Chem. Rev.* **2015**, *115*, 12320; h) K. I. Assaf, W. M. Nau, *Chem. Soc. Rev.* **2015**, *44*, 394.
[10] a) K. Kim, *Chem. Soc. Rev.* **2002**, *31*, 96; b) D. Tuncel, Ö. Ünal, M. Artar, *Isr. J. Chem.* **2011**, *51*, 525; c) X. Hou, C. Ke, J. Fraser Stoddart, *Chem. Soc. Rev.* **2016**, *45*, 3766.
[11] B. C. Pemberton, R. Raghunathan, S. Volla, J. Sivaguru, *Chem. Eur. J.* **2012**, *18*, 12178.
[12] a) S. Funk, J. Schatz, *J. Inclusion Phenom.* **2019**, *96*, 1; b) H. Barbero, E. Masson, *Cucurbiturils and Related Macrocycles* (Ed.: K. Kim), The Royal Society of Chemistry **2019**, Ch. 5, pp. 86–120.
[13] W. L. Mock, T. A. Irra, J. P. Wepsiec, T. L. Manimaran, *J. Org. Chem.* **1983**, *48*, 3619.
[14] W. L. Mock, T. A. Irra, J. P. Wepsiec, M. Adhya, *J. Org. Chem.* **1989**, *54*, 5302.
[15] P. Carlqvist, F. Maseras, *Chem. Commun.* **2007**, 748.
[16] D. Tuncel, J. H. G. Steinke, *Chem. Commun.* **2002**, 496.
[17] M. K. Sinha, O. Reany, M. Yefet, M. Botoshansky, E. Keinan, *Chem. Eur. J.* **2012**, *18*, 5589.
[18] a) D. Tuncel, J. H. G. Steinke, *Chem. Commun.* **1999**, 1509; b) D. Tuncel, J. H. G. Steinke, *Macromolecules* **2004**, *37*, 288.
[19] S. C. Han, J. Yoon, J. Oh, J. W. Lee, *Bull. Korean Chem. Soc.* **2011**, *32*, 3809.
[20] M. V. Rekharsky, H. Yamamura, M. Kawai, I. Osaka, R. Arakawa, A. Sato, Y. H. Ko, N. Selvapalam, K. Kim, Y. Inoue, *Org. Lett.* **2006**, *8*, 815.
[21] C. Yang, Y. H. Ko, N. Selvapalam, Y. Origane, T. Mori, T. Wada, K. Kim, Y. Inoue, *Org. Lett.* **2007**, *9*, 4789.
[22] C. Ke, R. A. Smaldone, T. Kikuchi, H. Li, A. P. Davis, J. F. Stoddart, *Angew. Chem. Int. Ed.* **2013**, *52*, 381.
[23] Y. Deng, X. Ren, M. P. Tang, S. K.-M. Lai, A. W. H. Ng, C.-N. Li, H. Y. Au-Yeung, *Mater. Today Chem.* **2022**, *24*, 100952.
[24] J. Y. H. Man, H. Y. Au-Yeung, *Beilstein J. Org. Chem.* **2019**, *15*, 1829.
[25] R. Liu, Y. Zhang, W. Wu, W. Liang, Q. Huang, X. Yu, W. Xu, D. Zhou, N. Selvapalam, C. Yang, *Chin. Chem. Lett.* **2019**, *30*, 577.
[26] C. Ke, N. L. Strutt, H. Li, X. Hou, K. J. Hartlieb, P. R. McGonigal, Z. Ma, J. Iehl, C. L. Stern, C. Cheng, Z. Zhu, N. A. Vermeulen, T. J. Meade, Y. Y. Botros, J. F. Stoddart, *J. Am. Chem. Soc.* **2013**, *135*, 17019.
[27] X. Hou, C. Ke, C. Cheng, N. Song, A. K. Blackburn, A. A. Sarjeant, Y. Y. Botros, Y.-W. Yang, J. F. Stoddart, *Chem. Commun.* **2014**, *50*, 6196.
[28] a) G. Gil-Ramírez, D. A. Leigh, A. J. Stephens, *Angew. Chem. Int. Ed.* **2015**, *54*, 6110; b) H. Y. Au-Yeung, C.-C. Yee, A. W. Hung Ng, K. Hu, *Inorg. Chem.* **2018**, *57*, 3475.
[29] H. Y. Au-Yeung, Y. Deng, *Chem. Sci.* **2022**, *13*, 3315.
[30] A. W. H. Ng, C.-C. Yee, K. Wang, H. Y. Au-Yeung, *Beilstein J. Org. Chem.* **2018**, 8.
[31] A. W. H. Ng, C.-C. Yee, H. Y. Au-Yeung, *Angew. Chem. Int. Ed.* **2019**, *58*, 17375.
[32] A. W. H. Ng, Y. H. Leung, H. Y. Au-Yeung, *Org. Chem. Front.* **2021**, *8*, 2182.
[33] K. Wang, C.-C. Yee, H. Y. Au-Yeung, *Chem. Sci.* **2016**, *7*, 2787.
[34] A. W. H. Ng, S. K. Lai, C. Yee, H. Y. Au-Yeung, *Angew. Chem. Int. Ed.* **2022**, *61*, e202110200.
[35] E. Mileo, C. Casati, P. Franchi, E. Mezzina, M. Lucarini, *Org. Biomol. Chem.* **2011**, *9*, 2920.
[36] Z. Yan, Q. Huang, W. Liang, X. Yu, D. Zhou, W. Wu, J. J. Chruma, C. Yang, *Org. Lett.* **2017**, *19*, 898.
[37] D. Tuncel, N. Cindir, Ü. Koldemir, *J. Inclusion Phenom. Macrocyclic Chem.* **2006**, *55*, 373.
[38] a) D. Tuncel, Ö. Özsar, H. B. Tiftik, B. Salih, *Chem. Commun.* **2007**, 1369; b) D. Tuncel, M. Katterle, *Chem. Eur. J.* **2008**, *14*, 4110.
[39] D. Tuncel, H. B. Tiftik, B. Salih, *J. Mater. Chem.* **2006**, *16*, 3291.
[40] S. Angelos, Y.-W. Yang, K. Patel, J. F. Stoddart, J. I. Zink, *Angew. Chem. Int. Ed.* **2008**, *47*, 2222.
[41] M. Özkan, Y. Keser, S. E. Hadi, D. Tuncel, *Eur. J. Org. Chem.* **2019**, *2019*, 3534.
[42] A. Khaligh, R. Khan, D. D. Akolpoğlu Başaran, M. Özkan, D. Tuncel, *ACS Appl. Polym. Mater.* **2020**, *2*, 5726.
[43] X. Hou, C. Ke, C. J. Bruns, P. R. McGonigal, R. B. Pettman, J. F. Stoddart, *Nat. Commun.* **2015**, *6*, 6884.
[44] X. Yu, W. Liang, Q. Huang, W. Wu, J. J. Chruma, C. Yang, *Chem. Commun.* **2019**, *55*, 3156.
[45] J. A. Finbloom, C. C. Slack, C. J. Bruns, K. Jeong, D. E. Wemmer, A. Pines, M. B. Francis, *Chem. Commun.* **2016**, *52*, 3119.
[46] C. C. Slack, J. A. Finbloom, K. Jeong, C. J. Bruns, D. E. Wemmer, A. Pines, M. B. Francis, *Chem. Commun.* **2017**, *53*, 1076.
[47] J. A. Finbloom, K. Han, C. C. Slack, A. L. Furst, M. B. Francis, *J. Am. Chem. Soc.* **2017**, *139*, 9691.
[48] a) F. d'Orchymont, J. P. Holland, *Angew. Chem. Int. Ed.* **2022**, *61*, e202204072; b) F. d'Orchymont, J. P. Holland, *Chem. Sci.* **2022**, *13*, 12713.
[49] F. d'Orchymont, J. P. Holland, *J. Am. Chem. Soc.* **2023**, *145*, 12894.
[50] a) M. Denis, S. M. Goldup, *Nat. Chem. Rev.* **2017**, *1*, 0061; b) K. D. Hänni, D. A. Leigh, *Chem. Soc. Rev.* **2010**, *39*, 1240; c) J. D. Crowley, S. M. Goldup, A.-L. Lee, D. A. Leigh, R. T. McBurney, *Chem. Soc. Rev.* **2009**, *38*, 1530.
[51] a) G. De Bo, G. Dolphijn, C. T. McTernan, D. A. Leigh, *J. Am. Chem. Soc.* **2017**, *139*, 8455; b) S. D. P. Fielden, D. A. Leigh, C. T. McTernan, B. Pérez-Saavedra, I. J. Vitorica-Yrezabal, *J. Am. Chem. Soc.* **2018**, *140*, 6049; c) C. Tian, S. D. P. Fielden, G. F. S. Whitehead, I. J. Vitorica-Yrezabal, D. A. Leigh, *Nat. Commun.* **2020**, *11*, 744.
[52] S. R. Beeren, C. T. McTernan, F. Schaufelberger, *Chem* **2023**, *9*, 1378.

Manuscript received: April 4, 2023
Revised manuscript received: June 29, 2023
Accepted manuscript online: July 17, 2023

Version of record online: July 31, 2023